State of Oregon
Oregon Department of Geology and Mineral Industries
Brad Avy, State Geologist

OPEN-FILE REPORT O-20-09

GIS DATA AND METHOD FOR DETERMINING MAXIMUM-CONSIDERED LOCAL AND DISTANT TSUNAMI WAVE ARRIVAL DATA FOR THE OREGON COAST

By Laura L. S. Gabel[1], Fletcher O'Brien[2], and Jonathan C. Allan[1]

2020

[1]Oregon Department of Geology and Mineral Industries, Coastal Field Office, P.O. Box 1033, Newport, OR 97365
[2]Oregon Department of Geology and Mineral Industries, 800 NE Oregon Street, Suite 965, Portland, OR 97232

DISCLAIMER

This product is for informational purposes and may not have been prepared for or be suitable for legal, engineering, or surveying purposes. Users of this information should review or consult the primary data and information sources to ascertain the usability of the information. This publication cannot substitute for site-specific investigations by qualified practitioners. Site-specific data may give results that differ from the results shown in the publication.

WHAT'S IN THIS REPORT?

This report describes the approach taken to generate statewide tsunami wave arrival rasters developed for a maximum-considered local (Cascadia subduction zone source) and distant (eastern Aleutian Islands source) tsunami that will impact the Oregon coast. Raster data are provided as an Esri ArcGIS geodatabase.

Oregon Department of Geology and Mineral Industries Open-File Report O-20-09
Published in conformance with ORS 516.030

For additional information:
Administrative Offices
800 NE Oregon Street, Suite 965
Portland, OR 97232
Telephone (971) 673-1555
https://www.oregongeology.org/
https://www.oregon.gov/DOGAMI

TABLE OF CONTENTS

LIST OF FIGURES

GEOGRAPHIC INFORMATION SYSTEMS (GIS) DATA

See the digital publication folder for files.

Geodatabase is Esri® version 10.6 format. Metadata is embedded in the geodatabase and is also provided as separate .xml format files.

Oregon_Coast_Tsunami_Wave_Arrival.gdb
- Rasters:
  - TsunamiWaveArrival_XXL
  - TsunamiWaveArrival_AKMax

Metadata in .xml file format:

Each raster listed above has an associated, standalone .xml file containing metadata in the Federal Geographic Data Committee Content Standard for Digital Geospatial Metadata format.

ABSTRACT

The objective of this report is to describe the approach taken to generate statewide tsunami wave arrival rasters developed for a maximum-considered local (Cascadia subduction zone) and distant (eastern Aleutian Islands) tsunami that will impact the Oregon coast. These data may then be integrated into an online map viewer (e.g., the NANOOS tsunami evacuation web portal) for access by the public.

Wave arrival times for a Cascadia subduction zone XXL scenario and eastern Aleutian Islands AKmax scenario are determined at ~20 million nodes covering the Oregon coast using several criteria evaluated in MATLAB®. The local (XXL) tsunami starts toward shore at the moment the earthquake starts, but the shaking from the earthquake can last three to five minutes. Wave arrivals are timed from the start of the earthquake. The tsunami wave arrival time was defined as that point in time when the simulated tsunami water level exceeds the background MHHW level by 6 inches (15.2 cm). Known false or misleading arrival times occur for several reasons, including earthquake-induced water "sloshing" (especially in the distal ends of estuaries), topographic features like large mud flats, low energy water at the distal edges of inundation, data seams and, on the south coast, proximity to the subduction zone. Some of these issues are addressed during the GIS process by converting wave arrival point data into rasters. Other issues are identified but not resolved and remain in the final products. This report is intended to support the use and understanding of the tsunami wave arrival data generated for the Oregon coast.

1.0 INTRODUCTION

The objective of this project is to produce statewide tsunami wave arrival rasters developed for a maximum-considered local (Cascadia subduction zone) and distant (eastern Aleutian Islands) tsunami that will impact the Oregon coast. These data may then be integrated into an online map viewer (e.g., the Northwest Association of Networked Ocean Observing Systems [NANOOS] tsunami evacuation web portal, http://nvs.nanoos.org/TsunamiEvac) for access by the public. Knowing when local and distant source tsunamis will arrive along the Oregon coast is important for evacuation planning and helps enable communities evaluate mitigation options such as route improvements and/or vertical evacuation.

A Cascadia subduction zone (CSZ) earthquake will shake the coast for 3–5 minutes, creating a tsunami that will inundate the Oregon coast within tens of minutes (Priest and others, 2009; Witter and others, 2011). A distant tsunami generated in the eastern Aleutian Islands in Alaska (Oregon's nearest neighboring subduction zone) will reach the Oregon coast in about 4 hours with no preceding earthquake felt on the Oregon coast.

In fiscal years 2009 through 2012, the Oregon Department of Geology and Mineral Industries (DOGAMI), modeled tsunami inundation for the entire Oregon coast. This work led to the adoption of two evacuation zones, reflecting both maximum-considered distant (AKmax) and local (XXL) tsunami inundation scenarios (Priest and others, 2013g). Tsunami evacuation maps based on the two scenarios have been distributed widely on the Oregon coast through publication, web access (https://www.oregongeology.org/tsuclearinghouse/pubs-evacbro.htm), and community outreach. However, much work remains to both maintain and improve public awareness of the hazard. A small number of wave elevation and velocity time histories were delivered as a part of the original modeling effort (Priest and others, 2013a–f), but detailed wave arrival time online maps will support tsunami outreach efforts to specific audiences such as coastal residents and businesses, local governments, the maritime community, and the tourism industry.

Wave arrival times (XXL and AKmax) are determined at every model node (~20 million total) in the MATLAB® computing environment using a simple set of criteria: for wet nodes, the time associated with the first 0.5-foot rise in water level, and for dry nodes, the time when water first arrives. This method accurately calculates wave arrival about 80% of the time. False or misleading wave arrivals occur for several reasons, including geomorphic features like large mud flats, slow/shallow water at the distal edges of inundation, data seams and, on the south coast, proximity to the subduction zone. Some of these issues are addressed during the GIS process converting MATLAB point data into rasters. Other issues are not resolved and remain in the final products. However, they are almost exclusively limited to uninhabited areas like inside estuaries and remote sloughs. Because of the large number of nodes, the original tsunami modeling was separated into 10 project areas. We further divide the coast into 90 extents to keep file sizes relatively small. All steps of the wave arrival calculation process are done within these extents and merged at the end.

This publication provides the following:

1. Geodatabase containing statewide raster data of tsunami wave arrival for the XXL and AKmax scenarios
2. This report explaining the method for calculating wave arrival

2.0 CALCULATING WAVE ARRIVAL TIMES

2.1 Extract time history data from tsunami model results

Tsunami simulations use unstructured computational grids constructed from detailed bathymetric and topographic data, particularly lidar. Computational grid spacing for tsunami simulations varied from ~ 4 km (2.5 mi) at the CSZ source, ~ 140 m (460 ft) at 70 m (230 ft) water depth, ~ 50 m (164 ft) at 20 m (66 ft) water depth, to ~7 m (23 ft) at the coast and on land (Priest and others, 2010) and at critical shoreline features such as jetties. Because of the high resolution, the coast was divided into 10 project areas with separate tsunami simulations for each (**Figure 1**). All project areas contain nodes for the entire Oregon coast, but the density is relatively low except in the area of interest. This prevents edge effects (i.e., tsunami waves "bouncing" off project edges as if they are solid landforms) between project areas. Other differences between project areas, detailed by Priest and others (2013g), include the timestep at which tsunami activity is calculated. Early tsunami models on the south coast used a 10-second timestep. This turned out to be unnecessarily detailed and created more data than necessary; therefore, central and north coast modeling used a 40-second timestep. There are approximately 20 million nodes covering the entire Oregon coast. For each of those nodes, wave elevation and velocity are calculated at every timestep for 8–12 hours. This creates a very large volume of data (~12 TB), which can be efficiently stored only in binary form.

Extracting usable time series data from the master binary dataset requires selecting a geographic subset of nodes and a period of time. We use the tsunami inundation map (TIM) series extents (**Figure 1**, https://www.oregongeology.org/pubs/tim/p-TIM-overview.htm) to guide our model data extraction, with each TIM extent containing anywhere from 30,000 to 2 million nodes depending on the size of the inundation zone in that location. We minimized the time period as much as possible to keep file sizes down while still capturing first wave arrivals in the area. For a local event, open coast tsunami wave arrivals mostly occur within the first hour and much of the inundation zone is reached with 2 hours; a few remote (distal) areas require 3 hours. The eastern Aleutian Islands (AKmax) distant event reaches the Oregon coast approximately 3 hours 45 minutes after the start of the model run, and data for several additional hours must be extracted from the master binary dataset to capture inland tsunami arrival times that are as late as 7 hours after the Alaska earthquake.

The tsunami modeling uses a mean higher high water (MHHW) vertical datum and a global coordinate system (WGS84). Subsidence, a sudden lowering of the coast in response to the earthquake, is also accounted for in the modeling. Wave elevations are reported in meters. Wave arrival determination is not reliant upon subsidence nor the conversion between MHHW and a projected vertical datum (i.e., NAD83) because we examined the relative change in water levels over time for a stationary node.

Time series data are extracted in the form of ASCII text files containing node ID and wave elevation at each timestep for the amount of time requested for every node within the geographic extent of a TIM (Priest and others, 2013a–f). As an example, TIM Curr-04 (Port Orford) contains 321,930 nodes but only 124,000 are inundated by an XXL tsunami. The rest are outside the inundation zone or do not meet our wave arrival threshold (section 2.3 discusses this detail further). For each of those nodes, there is a wave elevation value every 10 seconds between the start of the earthquake (t = 0) and t = 1 hour, for a total of 360 values, totaling 44.6 million data points for one hour of model data for ~8 miles of coastline.

Figure 1. Map of Oregon coast showing TIM extents and tsunami project areas. (*left*) north coast from Columbia River to Cape Perpetua and (*right*) Florence to California border. TIM extents are DOGAMI Tsunami Inundation Map series extents (https://www.oregongeology.org/tsuclearinghouse/pubs-inumaps.htm).

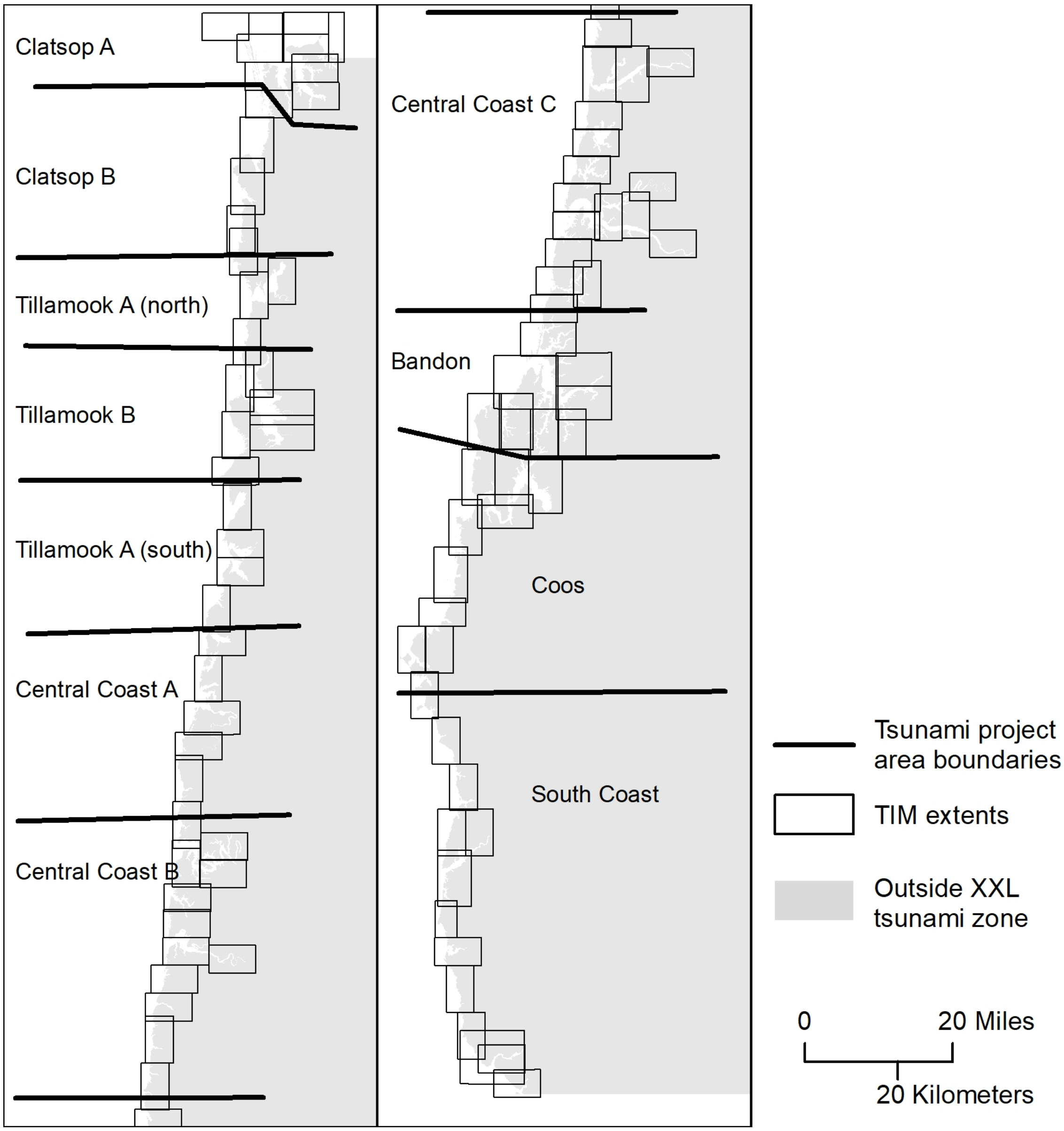

2.2 Calculate arrival time

Wave arrival is determined in MATLAB for each node using a simple set of guidelines meant to quickly process millions of nodes. For nodes on dry land, wave arrival is determined by the first timestep where data are present (**Figure 2**, ***left***). Prior to the arrival of the tsunami, wave elevation values for "dry" nodes are reported as "no data" or match the elevation of the ground surface (varies between project areas). For "wet" nodes over existing bodies of water such as the Pacific Ocean, estuaries, creeks, and lakes (regardless of their connectivity with the ocean), arrival is defined by a 0.5-foot (0.15 m) rise in the water level relative to the background tide level (i.e., MHHW at t = 0). The wet node example in **Figure 2**, ***right*** is in the shallow ocean, showing that the water elevation is 3.3 ft (2 m) below MHHW. This node indicates a withdrawal of water before the initial tsunami surge and occurs about 20 minutes after the earthquake begins. The water level rises 0.5 feet (0.15 m) above t = 0, ~27 minutes after the earthquake, and this is the value we report for the wave arrival at this location. We experimented with higher and lower thresholds before settling on 0.5 feet (0.15 m). Less than 0.5 feet (0.15 m) was too sensitive to non-wave arrival fluctuations (discussed further in section 3.2). Higher thresholds did better at ignoring some of those fluctuations; however, higher thresholds also missed some wave arrivals entirely. It takes several additional minutes for the peak of the first wave to arrive at open coast sites and up to several hours for inland sites.

Figure 2. Wave elevation time series and arrival times (green dots) for (left) a node on dry land, and (right) a node on an existing body of water (in this case, the Pacific Ocean). Note that the x-axis for dry node (left) does not start at zero.

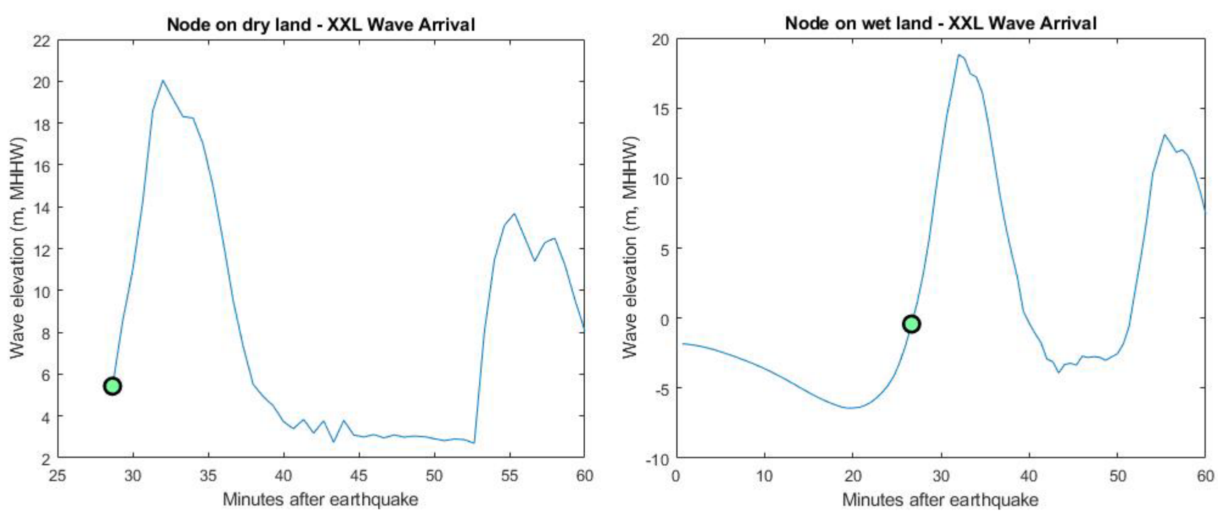

2.3 Mismatch between wave arrival raster and published inundation zones

The original inundation limits (Priest and others, 2013g) were determined by using a wet/dry parameter output from the hydrodynamic tsunami model based on a 1-cm (0.4 in) change in water level. Our wave arrival raster occasionally reports no wave arrival for an area despite being inside the inundation zone. This is because nodes in these areas have a change in water level greater than 0.4 inches but less than 6 inches. This only occurs at the distal ends of the tsunami inundation zone, mainly up estuary sloughs where the tsunami has run out of energy. This occurs in several estuary systems for XXL and nearly all for AKmax. The mismatch is noticeable when comparing wave arrival rasters to inundation zones at a large scale (i.e., when zoomed in), as shown in **Figure 3**, ***left*** (gap between datasets shown in white). **Figure 3**, ***right*** presents a time history for one of the final nodes that is inundated based on our method, showing a 1-ft (0.3 m) rise in water level. This reinforces the assumption that at this location, the tsunami is negligible in height and has little remaining energy; beyond this point there is no meaningful inundation. We found few cases where this issue directly affects populated areas because it mostly occurs in undeveloped tide lands. Even in populated areas, the phenomenon is restricted to a very narrow strip along the edge of the inundation zone.

Figure 3. Example of gap between wave arrival raster and inundation zone. In some areas, the tsunami runs out of energy prior to reaching reported edge of inundation. (*left*) Visual comparison of wave arrival raster and inundation zone showing tsunami model node locations. (*right*) Time history for actual edge of inundation zone showing small rise in water level.

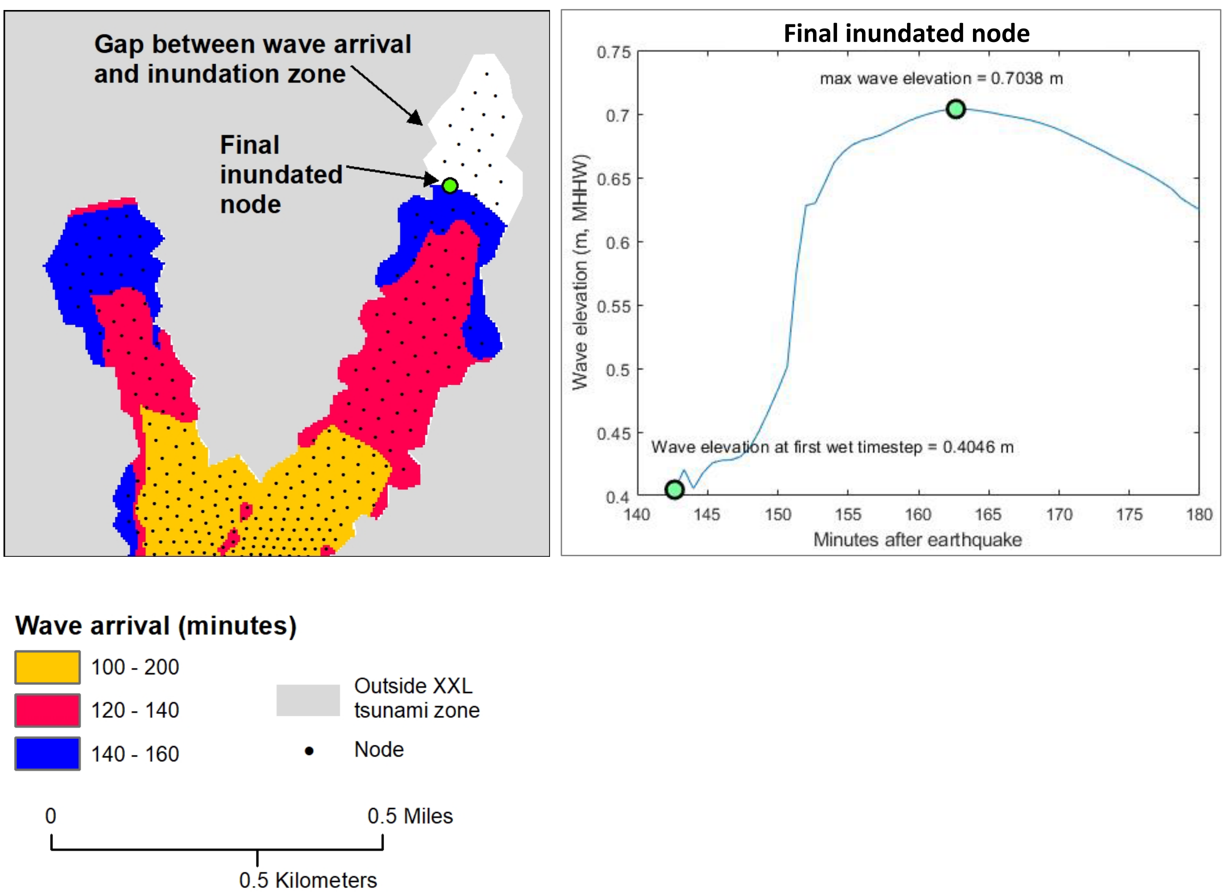

3.0 GIS PROCESSING

3.1 Method

A Python script developed by DOGAMI, which uses the Esri® ArcGIS® python library for the GIS processes, converts the ASCII wave arrival data into final GIS products. The steps are:

For each TIM extent:
1. Convert list of nodes with arrival times to a point feature class (WGS84)
2. Reproject points from WGS84 to NAD83
3. Generate raster by using the ArcGIS Natural Neighbor (20-ft [6 m] cell size) interpolation tool
4. Clip raster outside the inundation zone and outside the 3-nautical-mile state boundary

Statewide:
1. Mosaic together TIM rasters
2. Perform troubleshooting (discussed below)

3.2 Issues/troubleshooting

For many areas this method does not identify the correct wave arrival time. This is due to a few physical phenomena as well as peculiarities of the hydrodynamic model that are not identifiable with this method. The sheer number of nodes does not allow manual identification of arrival times for even small sections of the coast, but we developed several GIS workarounds to address the most egregious of cases. We focused on populated sections of coastline and did not edit the data in unpopulated areas.

Most difficulties arise from the earthquake shaking itself. This causes all bodies of water in the model to shake, or "slosh," starting at t = 0. This initial sloshing results in too-early wave arrivals in some locations for two reasons: First, the sloshing creates a seiche with amplitude > 0.5 foot (0.1 m). Second, a dry node very near the water can become wet from the shaking. We see this phenomenon along muddy estuarine shorelines as well as some jetties and levees. Sections 3.2.1 and 3.2.2 address our solutions to this issue. We also address several other issues, including confusing wave arrival data in some coastal lakes (section 3.2.3), early wave arrivals on the south coast due to proximity to the subduction zone (section 3.2.4), and data seams (section 3.2.5).

3.2.1 High frequency noise

The ArcGIS Spatial Analyst "Fill" tool is used to remove small regions of anomalous arrival times. This is akin to high-frequency noise in a generic dataset. **Figure 4** and **Figure 5** demonstrate an example of this correction along Netarts Spit in Tillamook County for a local XXL tsunami. **Figure 4**, ***top left*** shows the raw wave arrival raster with a thin line of early wave arrivals along the western shoreline of Netarts Bay. This portion of the bay is inundated 22 minutes after the earthquake. However, the strip of shoreline shows wave arrivals between 2 and 5 minutes after the earthquake. This is due to the initial earthquake-induced sloshing discussed above. **Figure 4**, ***top right*** shows the smoothed raster after the Fill tool has been applied. **Figure 5** presents time histories for neighboring nodes inside Netarts Bay; **Figure 5**, ***left*** for a dry node on the shoreline and ***right*** for a wet node in the bay. The overall pattern of inundation is identical between the two, but the shoreline node gets wet right away due to sloshing and incorrectly determines a 3-minute wave arrival. The Fill tool resolves most of these cases on jetties and levees, but in some cases the extent of the anomaly is too large, in which case we manually identify the correct wave arrival. This is discussed in the next section.

Figure 4. Example of early wave arrival removal in Netarts Bay, Oregon. (*top left*) Raw wave arrival calculations showing a strip of early arrivals along the western edge of the estuary shoreline. (*top right*) Final raster after Fill tool is applied. (*bottom left*) Aerial imagery of Netarts Spit for reference (2018 National Agriculture Imagery Program [NAIP] imagery).

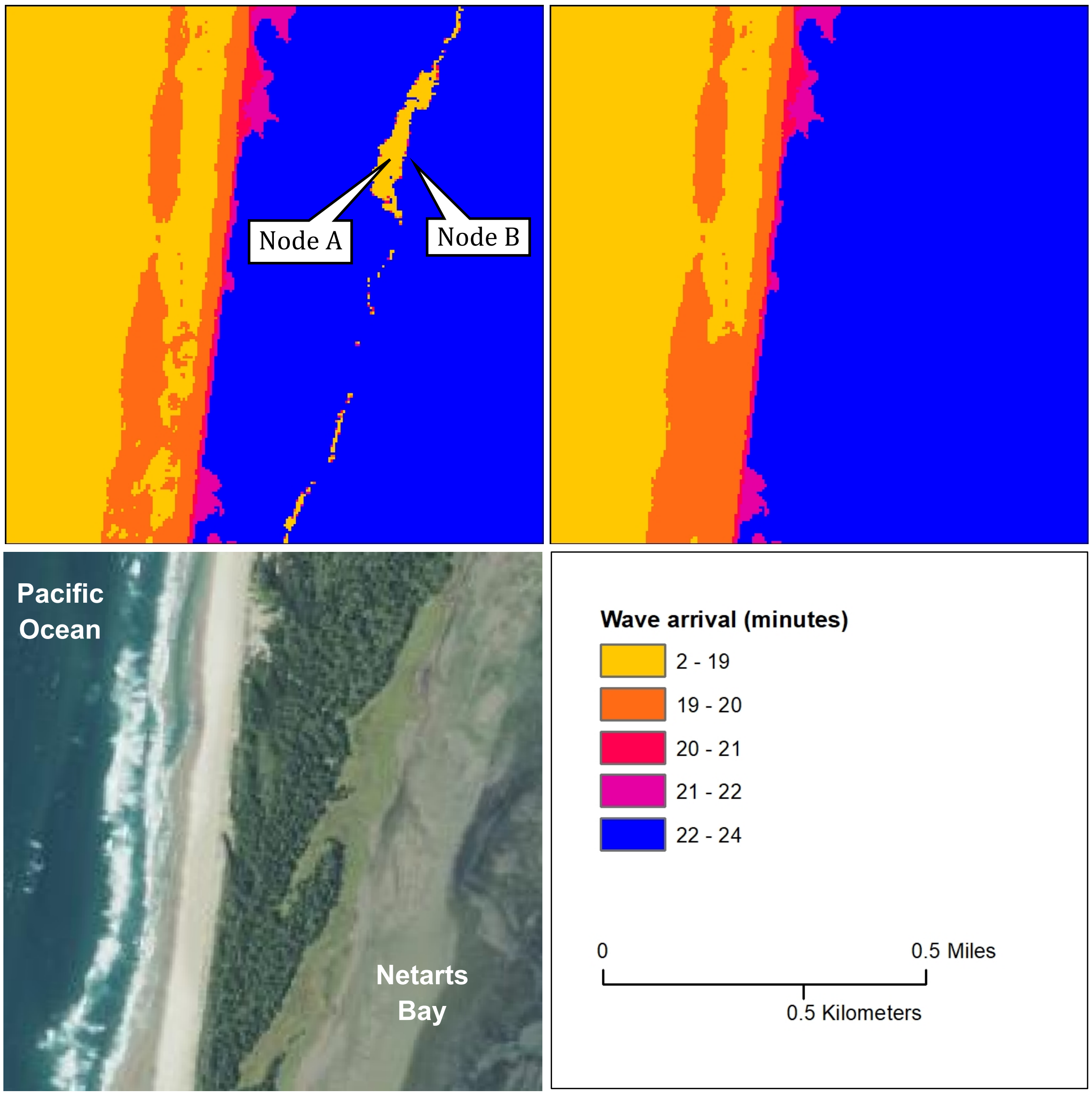

Figure 5. XXL wave elevation time histories for two nodes in Netarts Bay: (*left*) dry node on the shoreline and (*right*) for a wet node in the bay. See Figure 4-1, *top left* for node location.

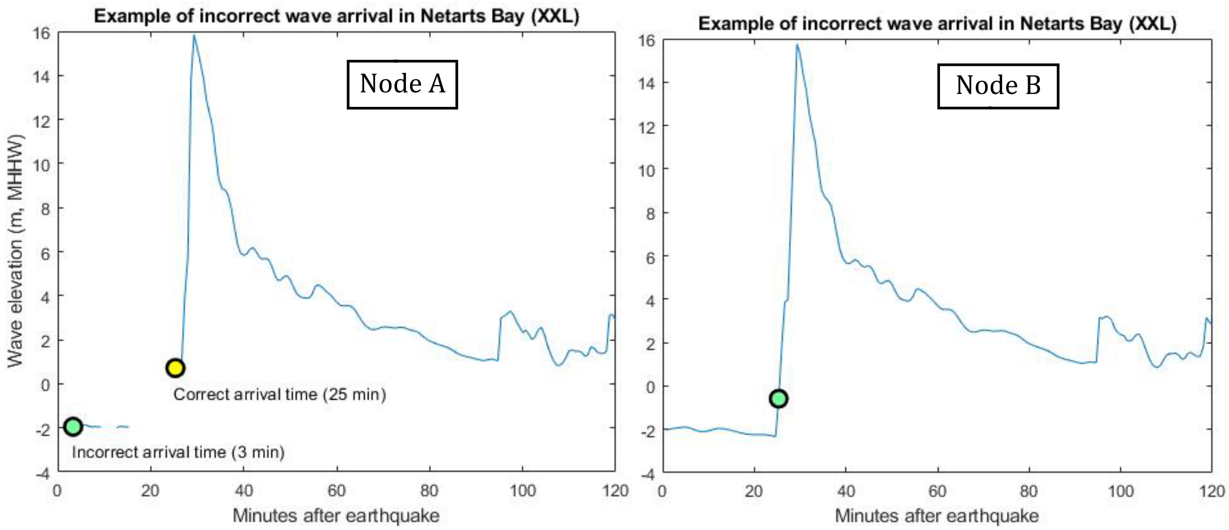

3.2.2 Interpolating across larger areas

The same earthquake-induced sloshing occurs on a much larger scale across mud flats in many of the major estuaries (local tsunami only). The mudflat nodes are wet at t = 0 and small ripples from the shaking are enough to trigger the 0.5-ft (0.15 m) threshold. These features are large and easy to spot upon visual inspection of the raw wave arrival raster (**Figure 6**, **top left**). Because we can see the broad pattern of inundation in the region and understand the topographic source of the issue (**Figure 6**, ***bottom left***), we considered it appropriate to remove the early wave arrival values by manually outlining their extents (shown in black) and interpolate the nearest values outside the area across it. **Figure 6**, ***top right*** shows the results after the interpolation.

Figure 6. Example of early wave arrival removal across mudflats in Coos Bay, Oregon. (*top left*) Raw wave arrival (*top right*) Final raster after early arrivals are identified and interpolated across boundaries. (*bottom left*) Aerial imagery of Coos Bay for reference (2018 National Agriculture Imagery Program [NAIP] imagery).

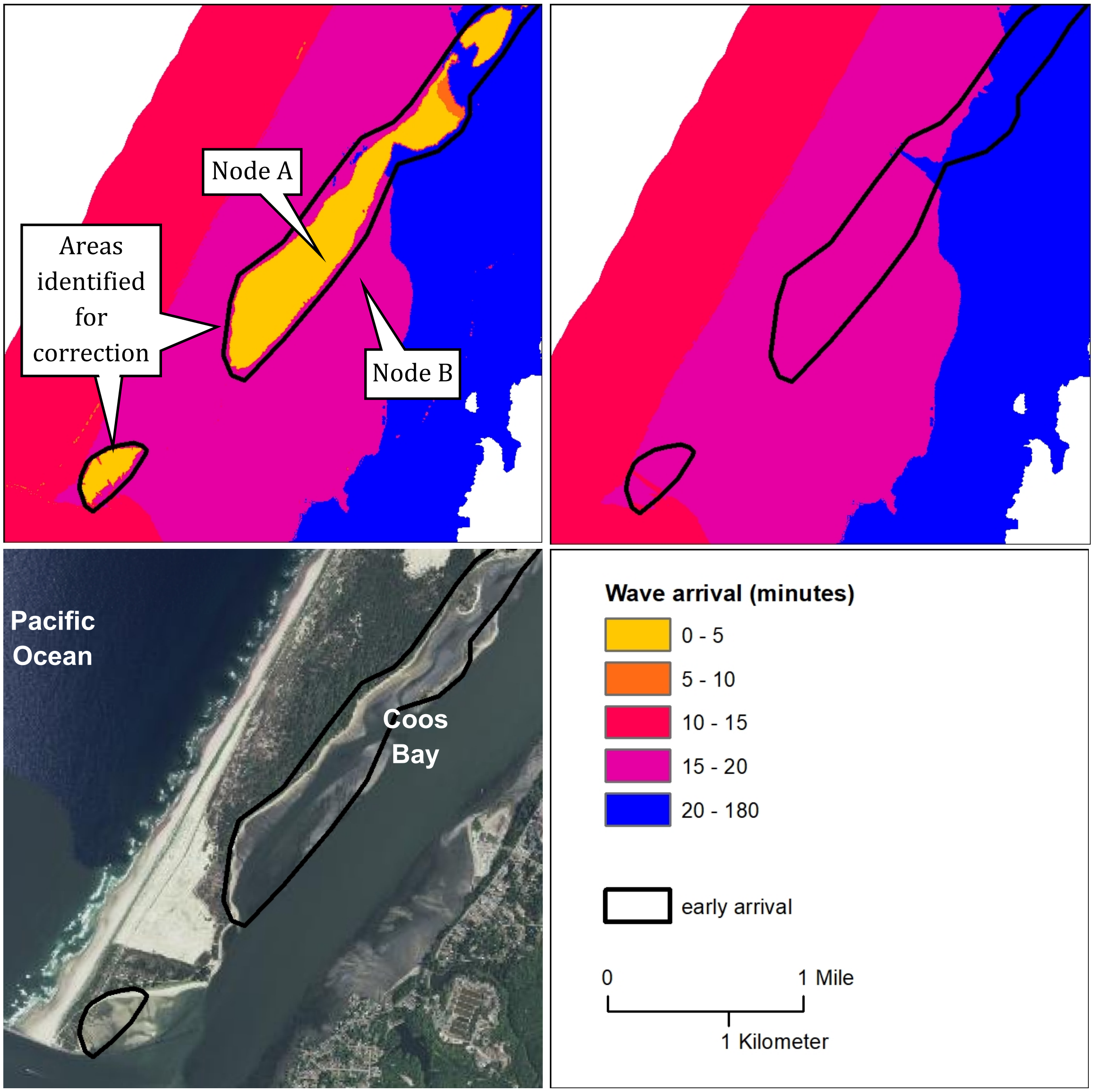

Figure 7 presents time histories for neighboring nodes inside the mouth of Coos Bay: **Figure 7**, ***left*** a node on a mudflat, and ***right*** a node in the adjacent river channel. The overall pattern of inundation is identical between the two, but the mudflat node incorrectly assigns a 2-minute wave arrival due to slightly higher sloshing than that experienced in the deeper river channel.

Figure 7. XXL wave elevation time histories for two nodes in Coos Bay: (*left*) node on a mudflat, and (*right*) node in adjacent river channel. See Figure 6, top left for node location.

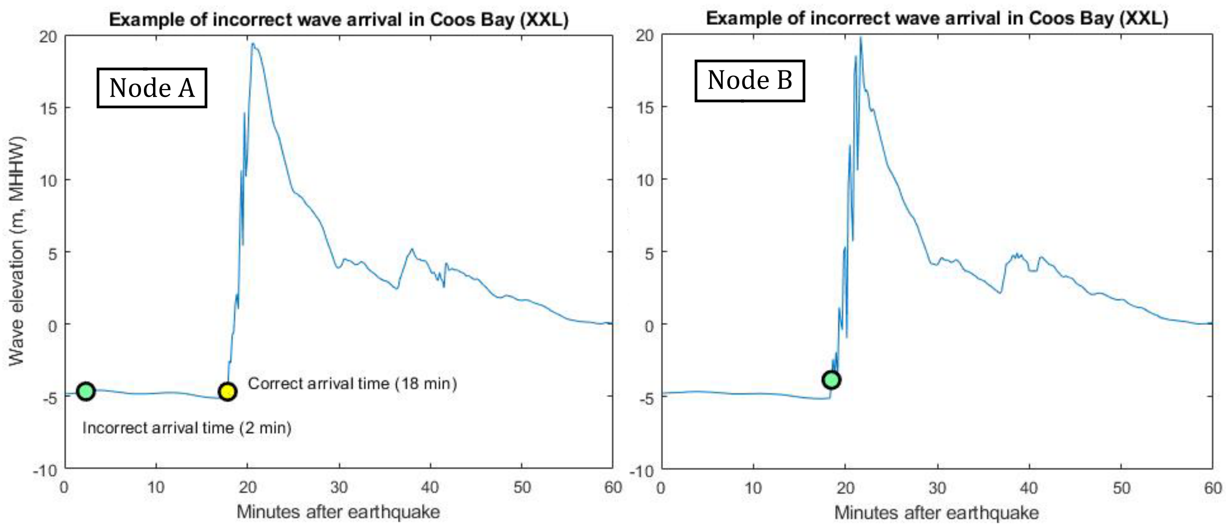

3.2.3 Coastal lakes

In evaluating the simulated XXL tsunami water elevations and velocities along the coast, we found several coastal lakes where the inundation zone may have over-reported the extent of inundation. Evidence for this includes wave arrivals that are significantly earlier than physically possible and unusual water elevation patterns. This discrepancy is primarily due to differences in how the tsunami modeler originally defined wet nodes and how we define them in this study. The original modeling identified any node in a water body as wet regardless of whether there is a change in water levels or not. Our method does not consider a node inundated if there is no change in water level due to the arrival of the tsunami. The other reason for our early wave arrivals is earthquake-induced seiching (i.e., “sloshing”), which creates small fluctuations in water levels that start at or near t = 0. Also see Section 2.3 for discussion on discrepancies between this dataset and the original inundation zones.

The most dramatic example is the XXL inundation in Tenmile Lake, between Reedsport and Coos Bay in Coos County (**Figure 8**). The same issue occurs in neighboring Tahkenitch and Siltcoos Lakes and the upper Coquille River Valley for local tsunami inundation; a similar problem was observed for the distant tsunami scenario in Lake Lytle, Rockaway Beach, Tillamook County. Each of these locations has topographic constraints that have a dissipative effect on tsunami energy. In the case of Tenmile Lake, the tsunami must travel ~3 miles over a large dune field, coastal forest, and then up along a narrow channel before entering the lake (**Figure 8**, ***top***). The raw wave arrivals show significantly earlier wave arrival times in the lake compared with wave arrivals along the tsunami inundation path, which is clearly incorrect (**Figure 8**, ***bottom***).

A series of wave elevation time histories following the XXL tsunami’s path to Tenmile Lake is shown in **Figure 9**. Station 1 demonstrates a “classic” first wave arriving after 28 minutes, and Stations 2 and 3 show how the leading edge of the tsunami has converted into a bore as it narrows along Tenmile Creek. Stations 4 through 9 demonstrate the range of time histories seen in Tenmile Lake. Stations 4 and 5 suggest the tsunami enters the lake as a ~3-ft (0.9 m) bore and by Station 7 has negligible height. Stations 5 through 8 show various levels of high-frequency oscillations in the water level time series, which we attribute to the arrival of attenuated tsunami waves (i.e., ripples). Oscillations have diminished by Station 9, which suggests that at this distance from the lake mouth, what little energy left in the tsunami has been disbursed across the broad shallow lake.

These time histories show that although all nodes within the lake experience the same early wave arrival problem seen on large mudflats, there is not a similar correction for the lake because it is unclear what the correct arrival times should be. There is a small but measurable water level rise at ~45 minutes for Stations 4 and 5, but that signal becomes much harder to discern with the naked eye and impossible to calculate using our 0.5-foot threshold beyond this point. For these reasons, we elected to remove all wave arrival data beyond the lake outlet. Early arrivals inside the channel just before the outlet were adjusted manually in a method described in section 3.2.1.1. The inundation zone in this area covers only the lake itself plus a narrow strip of shoreline. The raster will show a maximum arrival time of 35 minutes in this area, which can be used for the greater Tenmile Lake area for evacuation planning purposes.

Figure 8. Raw wave arrivals in Tenmile Lake system for XXL tsunami scenario. (*top*) Aerial image of Tenmile Creek leading to Tenmile Lake by the town of Lakeside. Green color shows the area outside XXL tsunami zone. (*bottom*) Early wave arrivals in the lake are incorrect and are ultimately removed from the final wave arrival raster. Base map is 2018 National Agriculture Imagery Program (NAIP) imagery; the XXL inundation zone (non-green area) on this and following figures is from Priest and others (2013g).

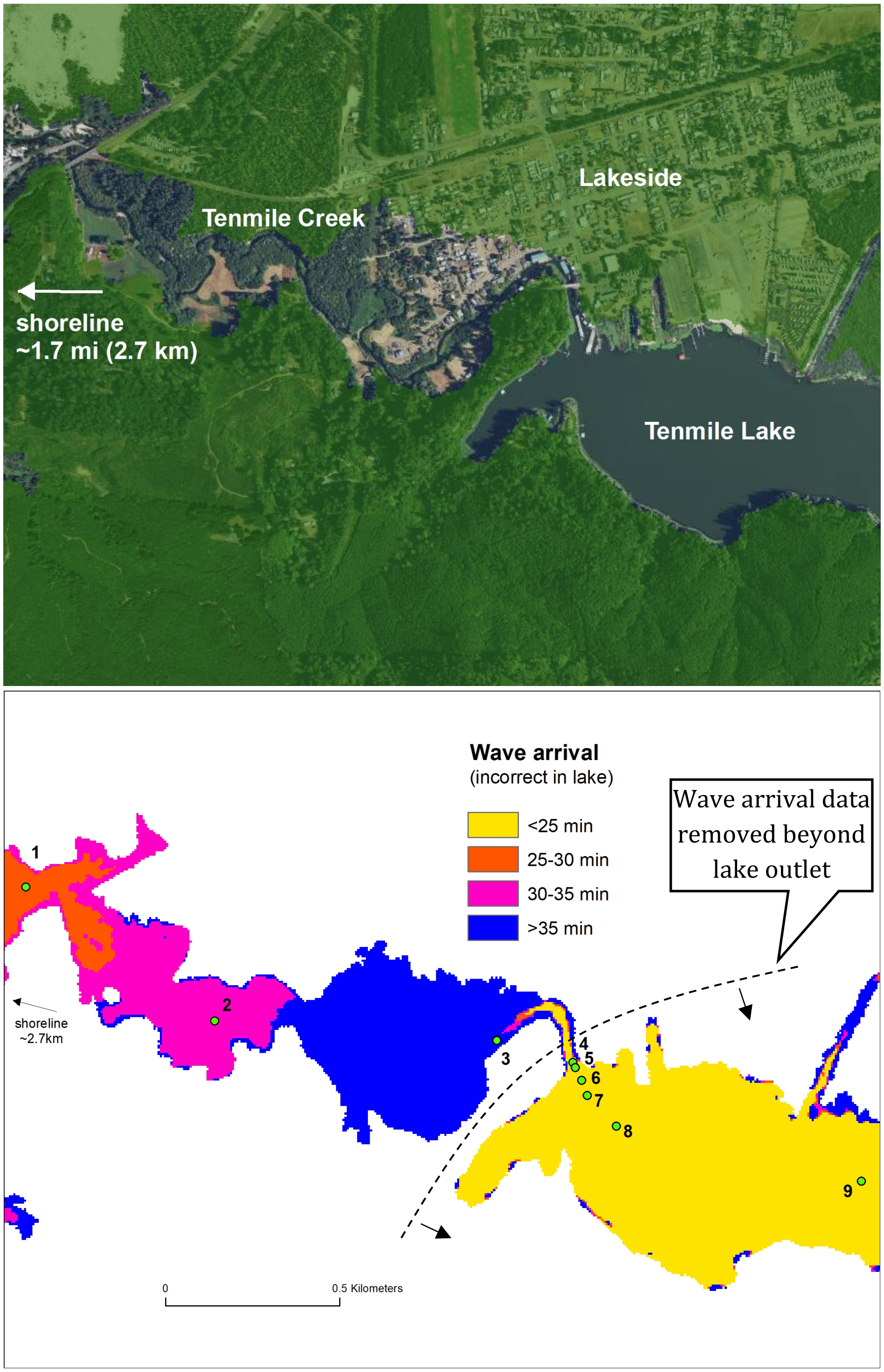

Figure 9. XXL wave elevation time histories for multiple nodes in Tenmile Lake system (see Figure 8, bottom for node locations). (*top*) Stations 1–9 with a y-axis of +6 to −3 m above MHHW. (*bottom*) Stations 4–9 with a y-axis of −0.5 to −3 m above MHHW to examine small fluctuations in water levels in the lake.

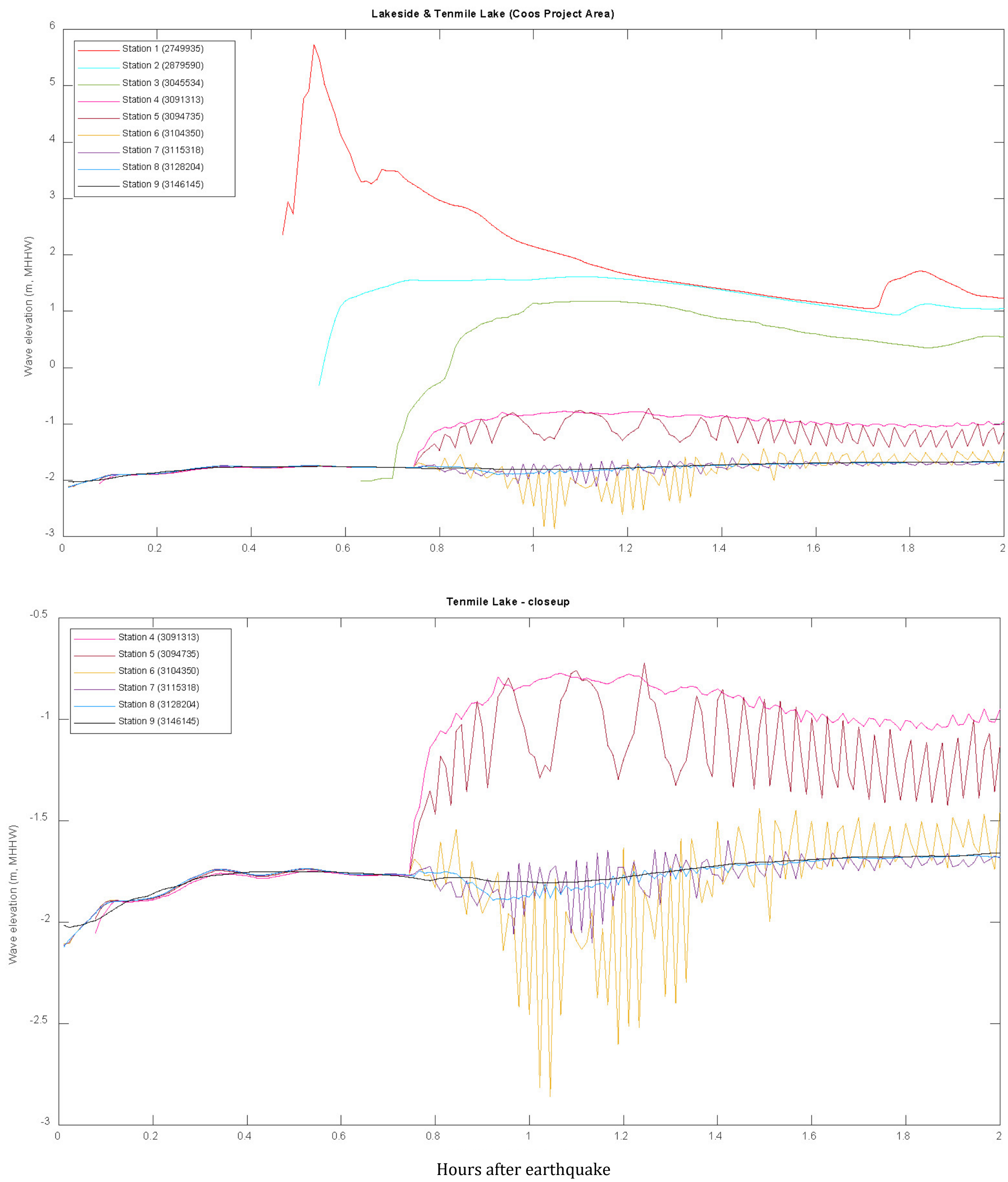

3.2.4 South coast early wave arrivals

The proximity of the coastline to the Cascadia subduction zone in the south results in significantly earlier wave arrivals than what is calculated for the central and north coast (local tsunami only). Not only does the tsunami have less distance to travel, but the initial column of water lifted by the seafloor triggers the 0.5-foot threshold after only a few minutes even if the first peak does not arrive for several additional minute. **Figure 10** presents XXL wave arrivals for the southern Oregon coast (from Siuslaw River at Florence south to Brookings), highlighting wave arrivals *on the beach* and the coastline's proximity to the subduction zone. The earliest calculated beach arrivals are between Bandon (Coquille River) and Port Orford (0–5 minutes). This zone includes Cape Blanco, the westernmost point in Oregon and the closest point of land to the subduction zone. Between Bandon and Cape Arago to the north and between Port Orford and Brookings to the south, beach arrival times increase to 5–10 minutes. There is a further delay in arrival times (10–15 minutes) in the Coos Bay area, and beach arrival times of 15–25 minutes for the remainder of the Oregon coast.

Another feature causing earlier wave arrivals in this area is the presence of the Rogue submarine canyon, which focuses the tsunami toward Cape Blanco and allows the tsunami to retain more of its energy as it approaches the coastline. This allows the tsunami to retain more of its deep-water speed compared to adjacent locations on the continental shelf, so the tsunami reaches the shoreline more quickly.

Figure 10. XXL tsunami wave arrivals for the southern Oregon coast, highlighting arrival times on the beach and the proximity of the coast to the subduction zone.

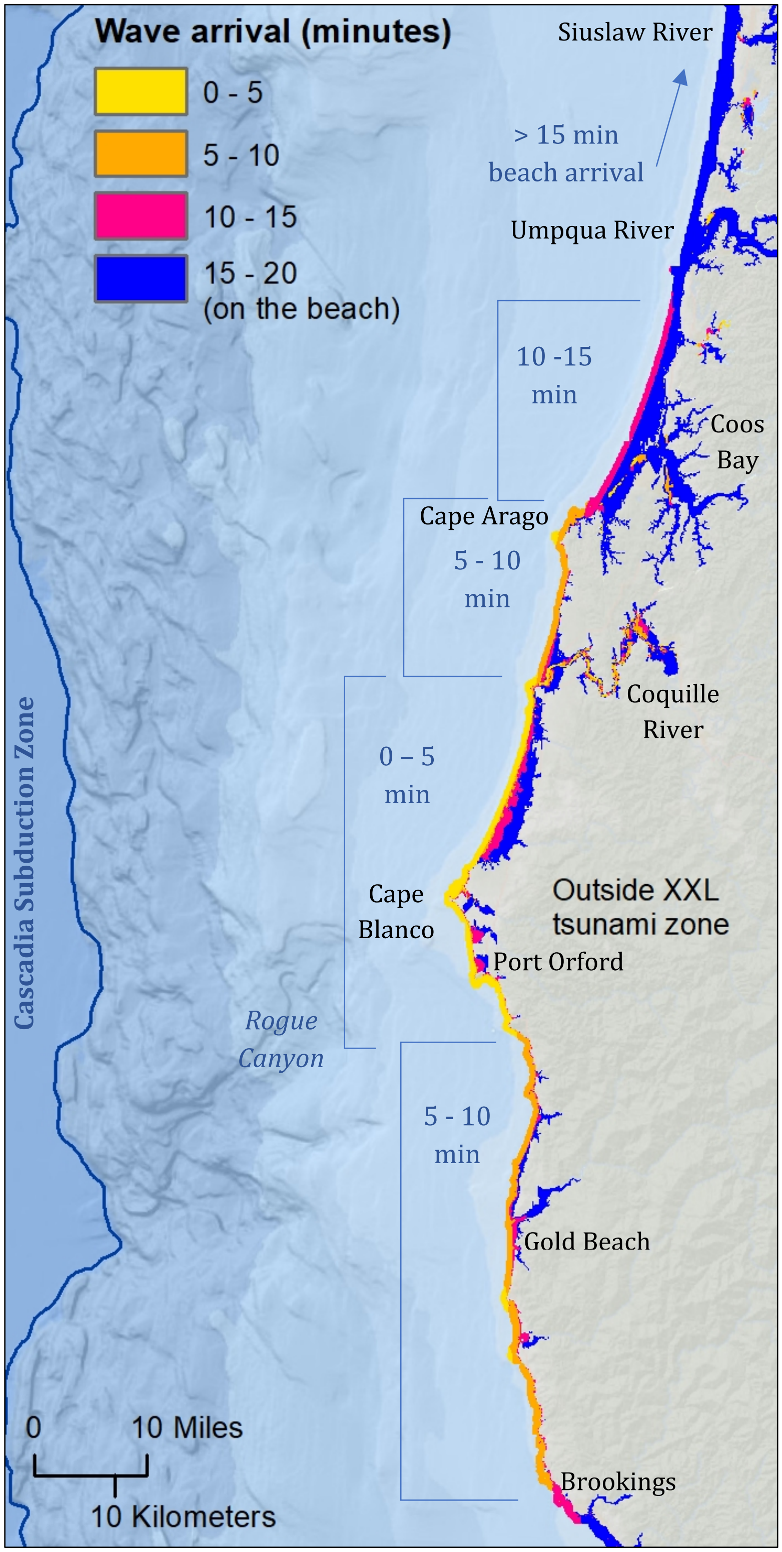

Base map: Esri "World Ocean Base" and "World Topographic Map," 2019. https://www.bodc.ac.uk/data/hosted_data_systems/gebco_gridded_bathymetry_data/. (Accessed August 12, 2020)

3.2.4.1 Coquille River

Time series data in the Coquille River appear to be especially susceptible to the south coast early wave arrival issue, with our threshold reporting anomalously early arrivals throughout the length of the estuary, even 20 miles upriver by the town of Coquille. **Figure 11**, ***top left*** shows early wave arrivals by the mouth of the Coquille River. The XXL tsunami reaches the beach in 5–10 minutes, but inside the jetty there are large swaths of 0–5 minute arrivals. The area with incorrect arrivals was identified and interpolated across, as described in section 3.2.2. The final raster is shown in **Figure 11**, ***top right***. It is important to note that arrivals *on land* are correct; it is only within the river and flood plains that we see this phenomenon. **Figure 11**, ***bottom right*** shows wave elevation time histories for two nodes: Node A in the river channel and Node B in Old Town, Bandon. Node A experiences a 0.5-ft rise in water level very early due to the south coast issues previously discussed, and the wave arrival is reported as ~4 minutes. The node on dry land does not see an increase in water levels until ~14 minutes. A visual comparison of the two plots shows general agreement in wave arrival time, around 12–14 minutes.

Figure 11. Early wave arrivals in the lower Coquille estuary. (*top left*) Raw wave arrival, and (*top right*) final raster after early arrivals are identified and interpolated across boundaries. (*bottom left*) Aerial imagery of lower Coquille estuary, including the City of Bandon, for reference (2018 National Agriculture Imagery Program {NAIP} imagery). (*bottom right*) XXL wave elevation time histories for two nodes in lower Coquille estuary.

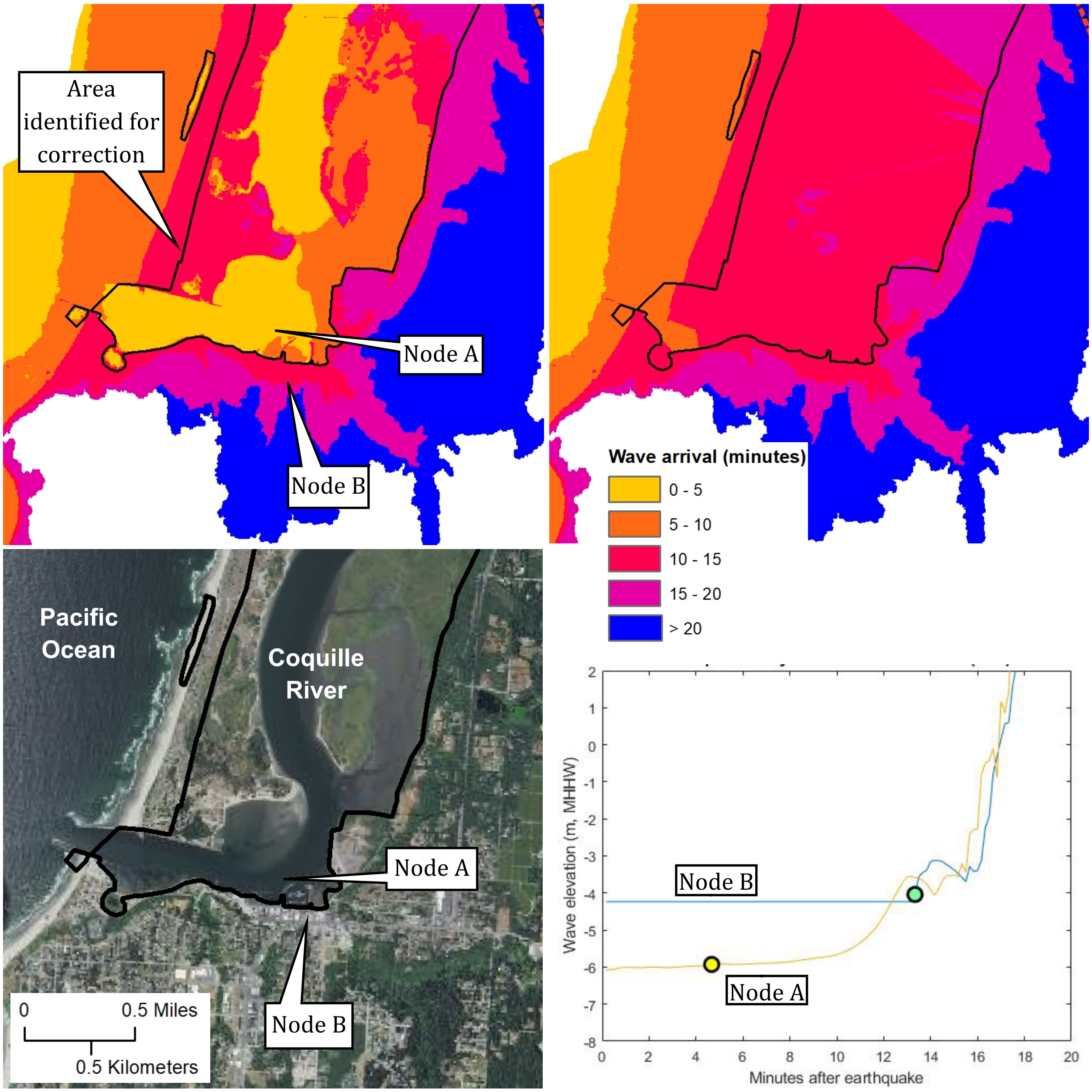

Because of the complex wave arrivals in the Coquille River (**Figure 12**, ***top left***), we developed a GIS workaround to create a final raster that reflects the correct overall wave arrivals upstream from Bandon and Highway 101. We examined individual time series plots and visually identified the time of wave arrival at ~30 locations along the river. We then used these values to create a new wave arrival raster for this section of river channel, where values were interpolated bewteen each of the 30 points. **Figure 12**, ***top left*** shows the raw XXL wave arrival raster for the Coquille estuary, the boundary beyond which all raw data were removed, and an example of three locations used to determine actual wave arrival times. **Figure 12**, ***bottom*** shows the time series data for three example nodes used to manually identify the correct wave arrival. The resulting final raster, including interpolation across early arrivals in the lower estuary as previously discussed, is shown in **Figure 12**, ***top right***.

Figure 12. Early wave arrivals in the Coquille estuary. (*top left*) Raw XXL wave arrival raster. (*top right*) Final raster after early arrivals removed and manual arrival times assigned upstream of Highway 101. (*bottom*) XXL wave elevation time histories for three sample nodes along the Coquille River. Green dots indicate raw wave arrival determination, yellow dots indicate manual wave arrival determination.

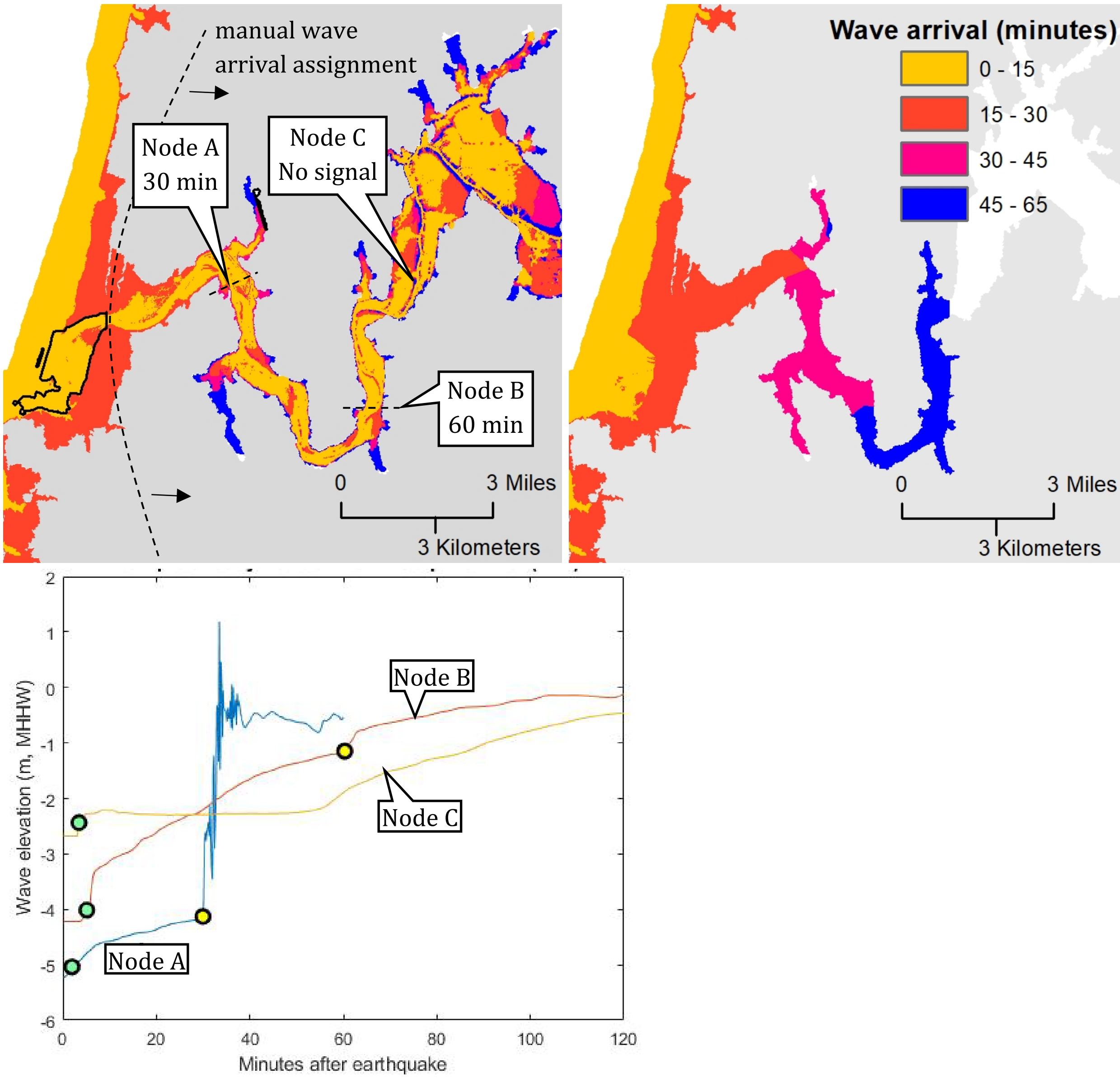

3.2.5 Data seams

Because the tsunami modeling divided the coast into 10 discrete project areas (**Figure 1**) and we ran scenarios for each area individually, there are some inevitable inconsistencies in tsunami wave arrival times across project boundaries. Although edge effects were accounted for in the original tsunami modeling (see section 2.1), small differences in the shape of the tsunami wave in some border areas resulted in the arrival threshold being triggered at slightly different times. For most of the Oregon coast there is complete agreement. However, in a few areas (offshore as well as within estuaries) there are visible seams in the raster. **Figure 13** demonstrates an example of this by Cape Falcon, Tillamook County, for AKmax. We chose not to modify the data in these areas.

Figure 13. Example of a wave arrival data seam between two tsunami model project areas for the AKmax scenario.

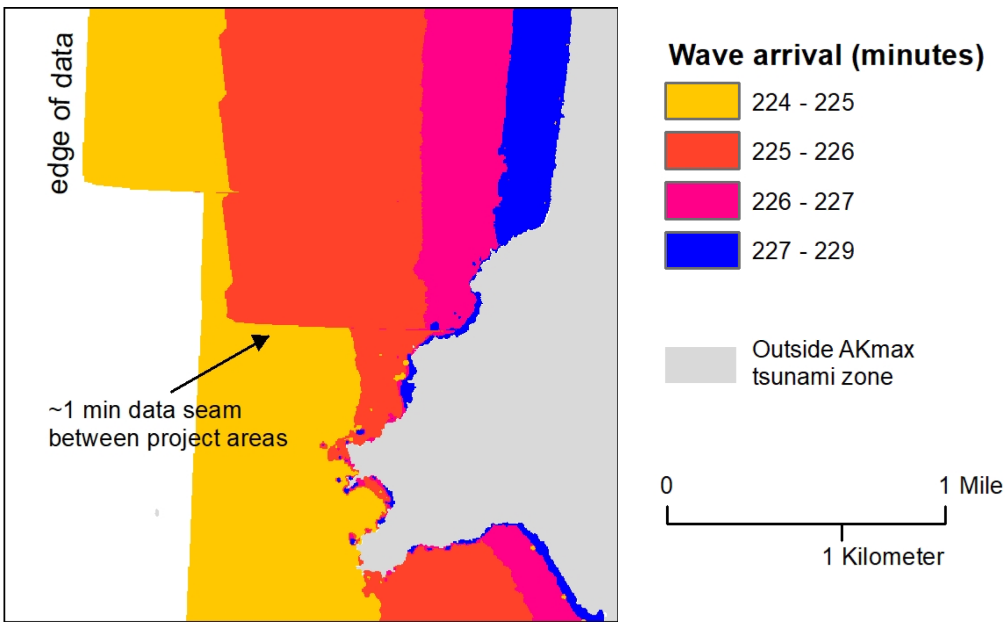

4.0 CONCLUSIONS

This project provides statewide wave arrival rasters for a maximum-considered local (XXL) and distant (AKmax) tsunami striking the Oregon coast. These data be integrated into an online map viewer (e.g., the NANOOS tsunami evacuation web portal) for access by the public. Knowing when local and distant source tsunamis will arrive along the Oregon coast is important for evacuation planning and helps enable communities evaluate mitigation options such as route improvements and/or vertical evacuation.

5.0 ACKNOWLEDGMENTS

This project was funded by the National Oceanic and Atmospheric Administration (NOAA) through the National Tsunami Hazard Mitigation Program under awards NA17NWS4670013 and NA18NWS4670076. We acknowledge the assistance of Robert Houston and Carlie Duda, DOGAMI, for careful review of the report and GIS data.

6.0 REFERENCES

Priest, G. R., Goldfinger, C., Wang, K., Witter, R. C., Zhang, Y., and Baptista, A. M., 2009. Tsunami hazard assessment of the northern Oregon coast: A multi-deterministic approach tested at Cannon Beach, Clatsop County, Oregon: Oregon Department of Geology and Mineral Industries Special Paper 41, 87 p., GIS data. https://www.oregongeology.org/pubs/sp/SP-41.zip

Priest, G. R., Goldfinger, C., Wang, K., Witter, R. C., and Zhang, Y. J., 2010, Confidence levels for tsunami-inundation limits in northern Oregon inferred from a 10,000 year history of great earthquakes at the Cascadia subduction zone: Natural Hazards, v. 54, p. 27–73. https://doi.org/10.1007/s11069-009-9453-5

Priest, G. R., Witter, R. C., Zhang, Y. J., Wang, K., Goldfinger, C., Stimely, L. L., English, J. T., Pickner, S. G., Hughes, K. L. B., Wille, T. E., and Smith, R. L., 2013a, Tsunami animations, time histories, and digital point data for flow depth, elevation, and velocity for the South Coast project area, Curry County, Oregon: Oregon Department of Geology and Mineral Industries Open-File Report O-13-13, GIS data. https://www.oregongeology.org/pubs/ofr/p-O-13-13.htm

Priest, G. R., Witter, R. C., Zhang, Y. J., Wang, K., Goldfinger, C., Stimely, L. L., English, J. T., Pickner, S. G., Hughes, K. L. B., Wille, T. E., and Smith, R. L., 2013b, Tsunami animations, time histories, and digital point data for flow depth, elevation, and velocity for the Bandon project area, Coos and Curry Counties, Oregon: Oregon Department of Geology and Mineral Industries Open-File Report O-13-14, GIS data. https://www.oregongeology.org/pubs/ofr/p-O-13-14.htm

Priest, G. R., Witter, R. C., Zhang, Y. J., Wang, K., Goldfinger, C., Stimely, L. L., English, J. T., Pickner, S. G., Hughes, K. L. B., Wille, T. E., and Smith, R. L., 2013c, Tsunami animations, time histories, and digital point data for flow depth, elevation, and velocity for the Coos Bay project area, Coos County, Oregon: Oregon Department of Geology and Mineral Industries Open-File Report O-13-15, GIS data. https://www.oregongeology.org/pubs/ofr/p-O-13-1.htm

Priest, G. R., Witter, R. C., Zhang, Y. J., Wang, K., Goldfinger, C., Stimely, L. L., English, J. T., Pickner, S. G., Hughes, K. L. B., Wille, T. E., and Smith, R. L., 2013d, Tsunami animations, time histories, and digital point data for flow depth, elevation, and velocity for the Central Coast project area, Coos, Douglas, Lane, and Lincoln Counties, Oregon: Oregon Department of Geology and Mineral Industries Open-File Report O-13-16, GIS data. https://www.oregongeology.org/pubs/ofr/p-O-13-16.htm

Priest, G. R., Witter, R. C., Zhang, Y. J., Wang, K., Goldfinger, C., Stimely, L. L., English, J. T., Pickner, S. G., Hughes, K. L. B., Wille, T. E., and Smith, R. L., 2013e, Tsunami animations, time histories, and digital point data for flow depth, elevation, and velocity for the Tillamook project area, Tillamook County, Oregon: Oregon Department of Geology and Mineral Industries Open-File Report O-13-17, GIS data. https://www.oregongeology.org/pubs/ofr/p-O-13-17.htm

Priest, G. R., Witter, R. C., Zhang, Y. J., Wang, K., Goldfinger, C., Stimely, L. L., English, J. T., Pickner, S. G., Hughes, K. L. B., Wille, T. E., and Smith, R. L., 2013f, Tsunami animations, time histories, and digital point data for flow depth, elevation, and velocity for the Clatsop project area, Clatsop County, Oregon: Oregon Department of Geology and Mineral Industries Open-File Report O-13-18, GIS data. https://www.oregongeology.org/pubs/ofr/p-O-13-18.htm

Priest, G. R., Witter, R. C., Zhang, Y. J., Wang, K., Goldfinger, C., Stimely, L. L., English, J. T., Pickner, S. G., Hughes, K. L. B., Wille, T. E., and Smith, R. L., 2013g, Tsunami inundation scenarios for Oregon: Oregon Department of Geology and Mineral Industries Open-File Report O-13-19, 14 p., GIS data. https://www.oregongeology.org/pubs/ofr/p-O-13-19.htm

Witter, R. C., Zhang, Y., Wang, K., Priest, G. R., Goldfinger, C., Stimely, L. L., English, J. T., and Ferro, P. A., 2011, Simulating tsunami inundation at Bandon, Coos County, Oregon, using hypothetical Cascadia and Alaska earthquake scenarios: Oregon Department of Geology and Mineral Industries Special Paper 43, 57 p., 3 pl., GIS files, animations. https://www.oregongeology.org/pubs/sp/p-SP-43.htm